

10-1-2009

The Vesicular Acetylcholine Transporter Is Required for Neuromuscular Development and Function

Braulio M. de Castro
Universidade Federal de Minas Gerais

Xavier De Jaeger
Western University; Universidade Federal de Minas Gerais

Cristina Martins-Silva
Western University

Ricardo D. F. Lima
Universidade Federal de Minas Gerais

Ernani Amaral
Universidade Federal de Minas Gerais

See next page for additional authors

Follow this and additional works at: <https://ir.lib.uwo.ca/anatomypub>

 Part of the [Anatomy Commons](#), and the [Cell and Developmental Biology Commons](#)

Citation of this paper:

de Castro, Braulio M.; De Jaeger, Xavier; Martins-Silva, Cristina; Lima, Ricardo D. F.; Amaral, Ernani; Menezes, Cristiane; Lima, Patricia; Neves, Cintia M. L.; Pires, Rita G.; Gould, Thomas W.; Welch, Ian; Kushmerick, Christopher; Guatimosim, Cristina; Izquierdo, Ivan; Cammarota, Martin; Rylett, Jane R.; Gomez, Marcus V.; Caron, Marc G.; Oppenheim, Ronald W.; Prado, Marco A. M.; and Prado, Vania F., "The Vesicular Acetylcholine Transporter Is Required for Neuromuscular Development and Function" (2009). *Anatomy and Cell Biology Publications*. 82.
<https://ir.lib.uwo.ca/anatomypub/82>

Authors

Braulio M. de Castro, Xavier De Jaeger, Cristina Martins-Silva, Ricardo D. F. Lima, Ernani Amaral, Cristiane Menezes, Patricia Lima, Cintia M. L. Neves, Rita G. Pires, Thomas W. Gould, Ian Welch, Christopher Kushmerick, Cristina Guatimosim, Ivan Izquierdo, Martin Cammarota, Jane R. Rylett, Marcus V. Gomez, Marc G. Caron, Ronald W. Oppenheim, Marco A. M. Prado, and Vania F. Prado

The Vesicular Acetylcholine Transporter Is Required for Neuromuscular Development and Function[∇]

Braulio M. de Castro,^{1†} Xavier De Jaeger,^{1,2,3†} Cristina Martins-Silva,^{2,3†} Ricardo D. F. Lima,⁴ Ernani Amaral,⁵ Cristiane Menezes,^{2,3} Patricia Lima,⁵ Cintia M. L. Neves,⁶ Rita G. Pires,² Thomas W. Gould,^{8‡} Ian Welch,⁹ Christopher Kushmerick,⁴ Cristina Guatimosim,⁵ Ivan Izquierdo,¹⁰ Martin Cammarota,¹⁰ R. Jane Rylett,^{2,3} Marcus V. Gomez,^{1,11} Marc G. Caron,¹² Ronald W. Oppenheim,⁸ Marco A. M. Prado,^{1,2,3,7*} and Vania F. Prado^{1,2,3,6,7*}

Programa de Farmacologia Molecular, UFMG, Belo Horizonte, Minas Gerais, Brazil¹; Molecular Brain Research Group, Robarts Research Institute,² and Department of Physiology and Pharmacology,³ University of Western Ontario, London, Ontario, Canada; Departamento de Fisiologia e Biofísica,⁴ Departamento de Morfologia,⁵ and Departamento de Bioquímica-Imunologia,⁶ UFMG, Belo Horizonte, Minas Gerais, Brazil; Department of Anatomy and Cell Biology, University of Western Ontario, London, Ontario, Canada⁷; Department of Neurobiology and Anatomy, Wake Forest University, Winston-Salem, North Carolina⁸; Animal Care and Veterinary Services, University of Western Ontario, London, Ontario, Canada⁹; Centro de Memoria, Instituto de Pesquisas Biomedicas, PUC-RS, Porto Alegre, Brazil¹⁰; Nucleo de Neurociencias, Faculdade de Medicina, UFMG, Belo Horizonte, Minas Gerais, Brazil¹¹; and Department of Cell Biology, Duke University, Durham, North Carolina¹²

Received 24 February 2009/Returned for modification 19 March 2009/Accepted 8 July 2009

The vesicular acetylcholine (ACh) transporter (VACHT) mediates ACh storage by synaptic vesicles. However, the VACHT-independent release of ACh is believed to be important during development. Here we generated VACHT knockout mice and tested the physiological relevance of the VACHT-independent release of ACh. Homozygous VACHT knockout mice died shortly after birth, indicating that VACHT-mediated storage of ACh is essential for life. Indeed, synaptosomes obtained from brains of homozygous knockouts were incapable of releasing ACh in response to depolarization. Surprisingly, electrophysiological recordings at the skeletal neuromuscular junction show that VACHT knockout mice present spontaneous miniature end-plate potentials with reduced amplitude and frequency, which are likely the result of a passive transport of ACh into synaptic vesicles. Interestingly, VACHT knockouts exhibit substantial increases in amounts of choline acetyltransferase, high-affinity choline transporter, and ACh. However, the development of the neuromuscular junction in these mice is severely affected. Mutant VACHT mice show increases in motoneuron and nerve terminal numbers. End plates are large, nerves exhibit abnormal sprouting, and muscle is necrotic. The abnormalities are similar to those of mice that cannot synthesize ACh due to a lack of choline acetyltransferase. Our results indicate that VACHT is essential to the normal development of motor neurons and the release of ACh.

Cholinergic neurotransmission has key functions in life, as it regulates several central and peripheral nervous system outputs. Acetylcholine (ACh) is synthesized in the cytoplasm by the enzyme choline acetyltransferase (ChAT) (16). Choline supplied by the high-affinity choline transporter (CHT1) is required to maintain ACh synthesis (52). A lack of ChAT (4, 35) or the high-affinity choline transporter (21) in genetically modified mice is incompatible with life. ACh plays an important role in wiring the neuromuscular junction (NMJ) during development (38, 43). Embryonic synthesis of ACh is fundamental for the development of proper nerve-muscle patterning at the mammalian NMJ, as ChAT-null mice present aberrant

nicotinic ACh receptor (nAChR) localization and increased motoneuron (MN) survival, axonal sprouting, and branching (4, 35).

The vesicular ACh transporter (VACHT) exchanges cytoplasmic ACh for two vesicular protons (37, 41). Previously reported electrophysiological studies showed that quantal size is decreased by vesamicol, an inhibitor of VACHT, but only in nerve terminals that have been electrically stimulated (19, 59, 60, 63). VACHT overexpression in developing *Xenopus* MNs increases both the size and frequency of miniature-end-plate currents (54). In *Caenorhabditis elegans*, mutations in VACHT affect behavior (65). Moreover, a decrease in VACHT expression has functional consequences for mammals, as mutant mice with a 70% reduction in the expression levels of this transporter (VACHT knockdown [KD^{HOM}] mice) are myasthenic and have cognitive deficits (47). Hence, vesicular transport activity is rate limiting for neurotransmission “in vivo” (18, 47).

Exocytosis of synaptic vesicle contents is the predominant mechanism for the regulated secretion of neurotransmitters (55). However, alternative mechanisms of secretion have been proposed (20, 56, 61). Quantal ACh release, comparable to that seen in developing nerve terminals, has been detected in

* Corresponding author. Mailing address: Molecular Brain Research Group, Robarts Research Institute, University of Western Ontario, P.O. Box 5015, 100 Perth Drive, London, Ontario N6A 5K8, Canada. Phone: (519) 663-5777, ext. 24888. Fax: (519) 663-3789. E-mail for Marco A. M. Prado: mprado@robarts.ca. E-mail for Vania F. Prado: vprado@robarts.ca.

† B.M.D.C., X.D.G., and C.M.-S. contributed equally to this work.

‡ Present address: Department of Basic Medical Sciences, Oceania University of Medicine, P.O. Box 232, Apia, Samoa.

[∇] Published ahead of print on 27 July 2009.

myocytes and fibroblasts in culture, which presumably do not express VACHT (14, 24). More recently, it was found that the correct targeting of *Drosophila* photoreceptor axons is disrupted in flies with null mutations in ChAT (64). Remarkably, the inactivation of VACHT did not produce the same result (64). The result suggests that the release of ACh during development is not dependent on VACHT, perhaps because it is nonvesicular or because vesicular storage can occur without VACHT.

To test if the VACHT-independent secretion of ACh has any physiological role in the mammalian nervous system, we generated a mouse line in which the VACHT gene is deleted. These mice lack the stimulated release of ACh from synaptosomes, die after birth, and show several alterations in neuromuscular wiring consistent with a severe decrease in the cholinergic input to muscles during development. These experiments indicate that VACHT has an important role in maintaining activity-dependent ACh release that supports life and the correct patterning of innervation at the NMJ.

MATERIALS AND METHODS

Generation of VACHT knockout mice. The isolation of a VACHT genomic clone was described elsewhere previously (47). This genomic clone was used to construct a gene-targeting vector in which we added LoxP sequences flanking the VACHT open reading frame (ORF) and the TK-Neo cassette. One LoxP sequence was added 260 bp upstream from the VACHT translational initiation codon, and a second LoxP was added approximately 1.5 kb downstream from the stop codon. The TK-Neo cassette was added immediately after the second LoxP and was followed by a third LoxP (S1). Note that this is a vector distinct from what we previously reported for the localization of the TK-Neo cassette (47). The linearized targeting vector was electroporated into J1 embryonic stem cells derived from 129/terSv mice, and selected embryonic stem cell clones harboring homologous recombination (determined by PCR and Southern blotting [not shown]) were injected into C57BL/6J blastocysts to produce chimeric mice. Germ line transmission was achieved, and mice were bred to C57BL/6J mice to produce heterozygote mutant mice (VACHT^{wt/flox}). Prior to breeding VACHT^{flox} mice to transgenic mice constitutively expressing Cre, we bred VACHT^{flox} mice with CaMKIIalpha-Cre mice (Cre expression is driven by a fragment of the CaMKIIalpha promoter, kindly donated by Scott Zeitlin [17]) in an attempt to generate brain region-specific conditional knockout mice (these will be reported elsewhere). However, we noted that the progeny of mating between VACHT^{wt/flox,cre+}-CaMKIIalpha males and VACHT^{wt/flox} females inherited a recombined floxed allele (VACHT-deleted allele, or VACHT^{del}). This allele would be identical to that obtained by crossing the VACHT^{flox} mice to Cre mice that constitutively express Cre. This recombination happened because there is ectopic expression of CaMKIIalpha-Cre in the testes, which can be detected by quantitative reverse transcription-PCR (data not shown). The presence of Cre within the testes allows the recombination of the floxed allele, probably during spermatogenesis, and therefore, the VACHT^{del} allele is transmitted to the progeny. The ectopic expression of Cre in the testes was also previously described for other Cre lines (e.g., synapsin-Cre [49]), indicating that this is likely to be a common phenomenon. We backcrossed the progeny (VACHT^{wt/del}) to C57BL/6J mice (N4) and confirmed that they were capable of germ line transmission for the VACHT^{del} allele. We then intercrossed VACHT^{wt/del} mice to generate VACHT^{del/del} mice, i.e., a potential homozygous VACHT-null mutant (see below). For comparison purposes, we also obtained ChAT-null mice as a kind gift from Kuo-Fen Lee and Fred H. Gage, Salk Institute (4).

Animals were housed in groups of three to five mice per cage in a temperature-controlled room with 12-h light–12-h dark cycles, and food and water were provided ad libitum. Unless otherwise stated, the experiments were always done using embryonic day 18.5 (E18.5) embryos. All studies were conducted in accordance with NIH guidelines for the care and use of animals and with approved animal protocols from the Institutional Animal Care and Use Committees at the Federal University of Minas Gerais and the University of Western Ontario.

Genotyping, Southern blotting, and sequencing. Genotyping by PCR was performed using tail DNA as a template. The set of three primers used were P1 (5'-TACTTGTCTGTCTGCTGCCTGTC-3'), P2 (5'-AAGGAGTTGGTTGGCCACAGTAAG-3'), and P4 (5'-TCATAGCCCCAAGTGGAGGG AGA-3').

Oligonucleotides P1 and P2 amplified a 247-bp fragment in the wild-type (wt) allele, while primers P4 and P2 amplified a 329-bp fragment in the *del* allele. The 329-bp fragment amplified by primers P4 and P2 was purified from agarose gel using the QIAquick gel extraction kit (Qiagen) and cloned into the pCR 2.1 vector using the TA cloning kit (Invitrogen). The sequence of the cloned fragment was determined by automated DNA sequencing.

For Southern blot analysis, genomic DNA was digested with the enzymes BamHI and SacI. Digested DNA was subjected to electrophoresis in a 1.5% agarose gel and transferred onto a nylon membrane. After UV cross-linking, DNA on the membrane was hybridized to the NdeI/PmeI VACHT DNA fragment (see Fig. 1 for the position of the probe fragment). Detection was done using the Alkphos direct labeling and detection system kit (GE) according to the manufacturer's instructions.

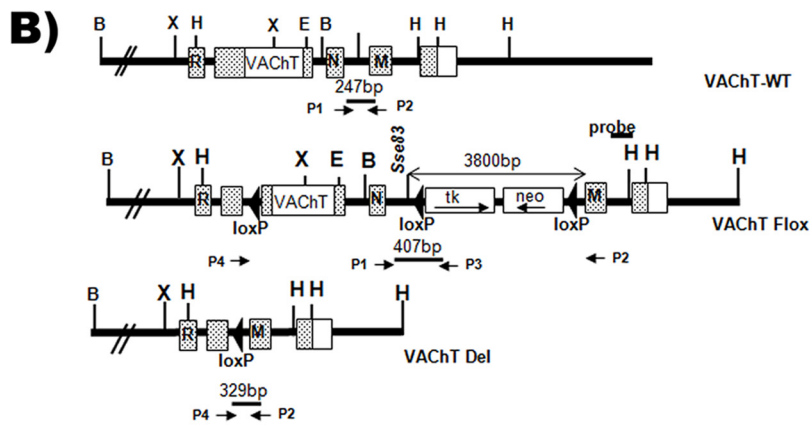
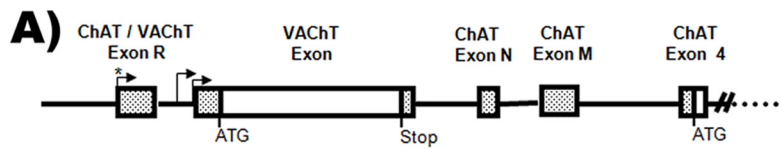
qPCR. For real-time quantitative PCR (qPCR), total RNA was extracted using Trizol (Invitrogen, São Paulo, Brazil) treated with DNase I (Ambion, Austin, TX), and first-strand cDNA was synthesized using a High Capacity cDNA transcription kit (Applied Biosystems, CA) according to the manufacturer's instructions. cDNA was subsequently subjected to qPCR on a 7500 real-time PCR system (Applied Biosystems, CA) using Power SYBR green PCR master mix (Applied Biosystems, CA). For each experiment, a nontemplate reaction was used as a negative control. In addition, the absence of DNA contaminants was assessed in reverse transcription-negative samples and by melting-curve analysis. The specificity of the PCRs was also confirmed by size verification of the amplicons by electrophoresis in acrylamide gels. Relative quantification of gene expression was done with the $2^{-\Delta\Delta CT}$ method using β -actin gene expression to normalize the data. The sequences of the primers used are available upon request.

Western blotting. Immunoblot analysis was carried out as described previously using spinal cord extracts from E18.5 mice (47). Antibodies used were anti-VACHT (Synaptic Systems Gottingen, Germany, and Sigma Chemical Co., São Paulo, Brazil), anti-CHT1 (51), anti-synaptophysin (Sigma Chemical Co.), and anti-actin (Chemicon, CA). Images were acquired and analyzed using ImageQuant TL (GE Healthcare).

Recombinant cDNA construct preparation, cell culture, and transfection. Rat CHT1 subcloned into the expression vector pcDNA3.1(-) and mutated in dileucine-like motif L531A was described previously (51). Human embryonic kidney HEK293 cells were acquired from the Cell Bank, Rio de Janeiro, Brazil. HEK293 cells were grown in Dulbecco's modified Eagle's medium (Gibco) supplemented with 10% (vol/vol) heat-inactivated fetal bovine serum (Gibco) and 1% penicillin-streptomycin (Gibco). For transient transfections with empty vector (pcDNA3.1) or mutant CHT1 (L531A), HEK293 cells were seeded into 60-mm dishes (Falcon) and transfected using a modified calcium phosphate method (23). Choline and ACh uptake assays were performed at 48 h after transfection.

Choline and ACh uptake assays and ACh release. Choline and ACh uptake assays were performed as described previously (50). Briefly, cells plated into 60-mm dishes were washed twice with Krebs-HEPES medium (124 mM NaCl, 4 mM KCl, 1.2 mM MgSO₄, 1 mM CaCl₂, 10 mM glucose, 25 mM HEPES [pH 7.4]) containing 10 mM paraoxon to inhibit acetylcholinesterase. Cells were then incubated with Krebs-HEPES containing 10 μ M paraoxon and [³H]choline chloride (1 μ M; diluted to 1 mCi/ μ mol) or [³H]ACh (1 mCi/ μ mol) for 10 min at 37°C. When hemicholinium-3 (1 μ M) was used, the drug was added during this incubation step and maintained during the course of the experiment. Subsequently, cells were washed three times with 1.0 ml of cold Krebs-HEPES with paraoxon (10 μ M) and lysed with 500 μ l of 5% trichloroacetic acid (TCA) solution. Lysates were centrifuged for 10 min at 10,000 \times g at 4°C. Pellets were used to measure protein content (3), and radioactivity was measured in the supernatants (100 μ l) by liquid scintillation spectrometry to determine choline and ACh uptakes. In the competition assay, choline uptake was performed in the presence of crescent amounts of ACh (3 mM, 10 mM, or 30 mM).

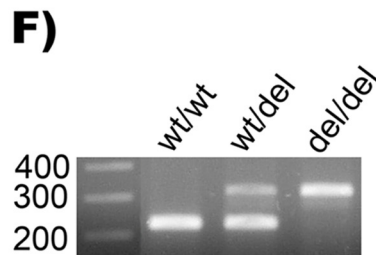
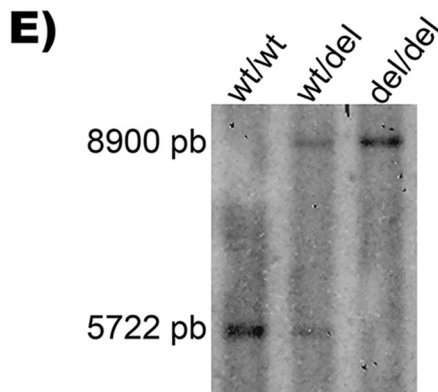
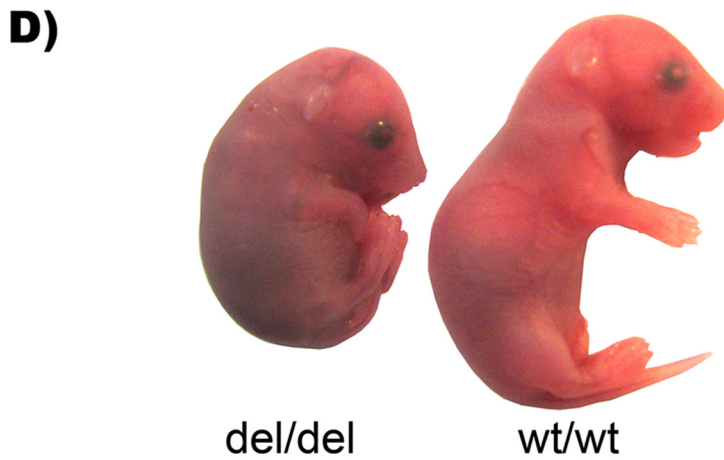
The TCA supernatants obtained as described above were used to determine the [³H]ACh content (45). Briefly, TCA was removed with ether, and quaternary amines were extracted using sodium tetraphenylboron in butyronitrile (10 mg/ml), the organic phase separated by centrifugation was reserved, and tetraphenylboron was precipitated with AgNO₃ in water. The suspension was homogenized and centrifuged. The organic phase was transferred into a new plastic tube containing MgCl₂ in water to precipitate excess Ag⁺. After centrifugation, the solution containing quaternary amines was taken to dryness under a vacuum. The [³H]choline present in dried samples was resuspended and oxidized using choline oxidase (Sigma-Aldrich) in glycylglycine buffer (pH 8). [³H]ACh was extracted using tetraphenylboron in butyronitrile similarly to the procedure described above. Tritium in the organic (predominantly ACh) and aqueous (corresponding predominantly to choline) phases was measured by liquid scintillation spectrometry.



C) DNA sequence of the VChT gene region. The sequence is shown in 60bp increments. Restriction sites for P4, AscI, and P2 are indicated. The loxP site is underlined in the 241-251bp region.

```

1  TCATAGCCCC AAGTGGAGGG AGAAAAAAAAA AAAAAAAGAG AGGCGGCGGT GGAGGAAGAG
   P4
61  GCAAGAGCGG ACGCGCGGGG AGGGCTGGAG AGACGGCGGG CGGCGGCAGC ATGCCCTGG
121 GCGGGTGCAC ACGGCCTCTC TGC GCGGCAG GGGCGGGCAG GGGCTGCTCC TGCTCTCTCT
181 GGGCACC GCGTCCAGTCT CCCGCCTCAG CCCCTCGGCT TGCCGGCCTA CTAGCATAAC
   NheI/SpeI
241 TTCGTATAAT GTATGCTATA CGAAGTTATG GCGCGCCCT GCAGGAATTG GATGGTAAAA
   loxP AscI
301 GAAAACAAGG GAGGTCTTAC TGTGGCCAAC CAACTCCTT
   P2
  
```



etry. Choline and ACh standards (0.1 to 0.5 $\mu\text{Ci/ml}$) were processed in parallel with the samples to assess yield and cross-contamination. The later values were used to correct results of sample analyses. Protein content determined by the method of Bradford was used to normalize the data (3). Choline or ACh uptake into cells that was dependent on CHT1 was measured as a percentage of transport in cells transfected with empty vector. Each n value represents the average of data for triplicate samples.

KCl-induced release of [^3H]ACh in brain synaptosomes. Crude synaptosomes from whole brains of individual mice were homogenized in ice-cold buffer (0.32 M sucrose, 10 mM EDTA, Tris-HCl [pH 7.4]), and P2 pellets were obtained as described previously (2), washed, and then incubated in a depolarizing solution (90 mM NaCl, 50 mM KCl, 5 mM NaHCO_3 , 1 mM MgCl_2 , 1.2 mM Na_2HPO_4 , 10 mM glucose, 20 mM HEPES, 2 mM CaCl_2 , 0.02 mM paraoxon [pH 7.4]) for 5 min at 30°C. Subsequently, samples were centrifuged at $5,500 \times g$ for 5 min at 4°C, and pellets were incubated in Krebs-HEPES medium (140 mM NaCl, 5 mM KCl) containing 100 nM of [^3H]choline, 5 mM NaHCO_3 , 1 mM MgCl_2 , 1.2 mM Na_2HPO_4 , 10 mM glucose, 20 mM HEPES, 2 mM CaCl_2 , and 0.02 mM paraoxon (pH 7.4) for 15 min at 30°C for choline uptake. After centrifugation, synaptosomes were washed three times with choline in ice-cold buffer (50 μM), and pellets were resuspended in ice-cold buffer. Each sample was separated into four aliquots. Two aliquots were incubated in Krebs-HEPES medium, and the other two aliquots were incubated in depolarizing solution containing hemicholinium-3 (1 μM) for 5 min at 30°C. The [^3H]ACh released was collected after centrifugation, pellets were digested with 5% TCA, and the radioactivity of both samples was measured using liquid scintillation counting. Total radioactivity (supernatant and pellet) was calculated and then normalized by protein content. For each sample, the average values obtained under depolarizing or nondepolarizing conditions was divided for the total radioactivity. The release of newly synthesized [^3H]ACh is predominant under this condition (2); the results are shown as fractional release above baseline release obtained under nondepolarizing conditions.

Tissue ACh measurements. Brains were dissected rapidly, homogenized in 5% TCA, and centrifuged ($10,000 \times g$ for 10 min) at 4°C. Supernatants were frozen at -80°C until use. For ACh determinations, TCA was removed with ether, and a chemiluminescent assay was done with choline oxidase as described previously (44). The data are presented as means and standard errors of the means (SEM). One-way analysis of variance (ANOVA), followed by Bonferroni's test, was used to analyze the differences in tissue ACh concentrations in $\text{VACHT}^{\text{wt/wt}}$, $\text{VACHT}^{\text{wt/del}}$, and $\text{VACHT}^{\text{del/del}}$ mice; a P value of <0.05 was considered to be statistically significant.

Electrophysiology. Electrophysiology experiments were performed similarly to methods described elsewhere previously (47). Hemidiaphragms were isolated from E18.5 embryos, and the muscle with attached nerve was pinned to a Sylgard pad in a 5-ml acrylic chamber continuously perfused at a rate of 1 ml/min with Tyrodes solution containing 137 mM NaCl, 26 mM NaHCO_3 , 5 mM KCl, 1.2 mM NaH_2PO_4 , 1.3 mM MgCl_2 , 2.4 mM CaCl_2 , and 10 mM glucose equilibrated with 95% O_2 –5% CO_2 at pH 7.4. During recording, tetrodotoxin (3 μM) was included to avoid contractions. Microelectrodes were fabricated from borosilicate glass and had resistances of 8 to 15 M Ω when filled with 3 M KCl. Standard intracellular recording techniques were used to record miniature end plate potentials with an Axoclamp-2A amplifier. Recordings were band-pass filtered (0.1 Hz to 10 KHz) and amplified 200 times prior to digitization and acquisition on an IBM computer running WinEDR (John Dempster, University of Strathclyde). The membrane potential was recorded and used to correct MEPP amplitudes and areas to a standard resting potential of -60 mV. At the end of experiments, 5 μM d -tubocurarine was applied to verify that the observed events were due to nicotinic receptors.

FM1-43 imaging. FM1-43 imaging experiments were performed as described previously (47) except that a fixable FM1-43 analog was used. Briefly, diaphragms from E18.5 mice were dissected and mounted onto a Sylgard-lined chamber containing mouse Ringer solution with the following composition: 135 mM NaCl, 5 mM KCl, 2 mM CaCl_2 , 1 mM MgCl_2 , 12 mM NaHCO_3 , 1 mM

Na_2HPO_4 , and 11 mM d -glucose. Solutions were aerated with 95% CO_2 –5% O_2 , and the pH was adjusted to 7.4. FM1-43fx (8 μM) was used to stain recycling synaptic vesicles during stimulus with a high- K^+ solution (60 mM KCl) for 10 min with 16 μM d -tubocurarine to prevent contractions. After stimulation, the preparation was maintained in normal K^+ solution for 10 min to guarantee maximal FM1-43fx uptake. Excess FM1-43fx adhering to the muscle cell plasma membrane was removed during a washing period in mouse Ringer solution not containing FM1-43fx for at least 40 min; 16 μM d -tubocurarine was present to prevent muscle contraction. Advasep-7 (1 mM) was added during the washing period after FM1-43fx staining to reduce background fluorescence. Diaphragms stained with FM1-43fx were fixed with 4% paraformaldehyde for 40 min and then mounted onto slides and examined by fluorescence microscopy on either an Axiovert 200 M microscope equipped with a 40 \times water immersion objective using the Apotome system or a Leica SP5 confocal microscope using a 63 \times water immersion objective and an argon laser (488 nm) for excitation. The spectrum emission was set from 510 to 620 nm. During image acquisition, whole hemidiaphragms were scanned, and the images were obtained from muscle areas with stained NMJs. The total number of junctions per hemidiaphragm was defined by the sum of junctions observed in each image after scanning the entire muscle. The density of junctions was determined by the ratio of the number of junctions/total area (mm^2). The nerve terminal area was measured using Image J, and the size of each terminal was expressed in pixels 2 . Data were analyzed using an unpaired t test. A P value of <0.05 was considered to be statistically significant.

Immunofluorescence. Immunofluorescence was performed as described previously (4). Briefly, whole-mount diaphragms from embryos were rapidly dissected and fixed in 4% paraformaldehyde–phosphate-buffered saline (PBS) (pH 7.4) for approximately 3 days. Tissues were cryoprotected with 10% sucrose–4% paraformaldehyde, frozen with isopentane over dry ice, and kept at -80°C until use. Muscles were rinsed two times in PBS, incubated with a 0.1 M glycine–PBS solution for 1 h, and blocked in incubation buffer (150 mM NaCl, 0.01 M phosphate buffer, 3% bovine serum albumin, 5% goat serum, and 0.01% thimerosal) overnight at 4°C. Tissues were immunostained with anti-VACHT (rabbit polyclonal; Sigma Chemical Co.), anti-CHT1 (51), or anti-neurofilament 150 (rabbit polyclonal; Chemicon) in incubation buffer overnight at 4°C. Following three washes of 1 h each with PBS–0.5% Triton X-100, muscles were incubated with Alexa Fluor 546-conjugated goat anti-rabbit antibody (Molecular Probes) and Alexa Fluor 488-conjugated α -bungarotoxin (Molecular Probes) in the buffer described above overnight at 4°C, and the washing step was repeated. Diaphragms were flat mounted in Hydromount medium, and images were collected with an Axiovert 200 M microscope using the Apotome system or a Leica SP5 confocal microscope to acquire optical sections of the tissues. Quantitative analyses of nAChR or CHT1 fluorescence were carried out with Metamorph software (Molecular Devices, Downingtown, PA). For each set of experiments, a threshold was calculated by using a background area of the image. This threshold value determined for $\text{VACHT}^{\text{wt/wt}}$ was applied to images obtained with other genotypes, and the total fluorescence intensity (integrated intensity) for bungarotoxin-labeled nAChR or terminals labeled by CHT1 antibody was then detected automatically. To count the number of positive terminals or junctions, adjacent sections of the entire muscle were obtained, and the numbers of positive labeled structures were counted with Metamorph similarly to the above-described experiments with FM1-43.

MN quantification. Adult pregnant females were anesthetized with ketamine-xylazine (70 mg/kg and 10 mg/kg, respectively) intraperitoneally and sacrificed by cervical dislocation. Embryos were removed quickly, and spinal cords were removed and immersed in Bouins fixative for 24 h prior to being processed for paraffin embedding. Paraffin blocks were serially sectioned, with sections placed onto microscope slides and stained with thionin. MNs were counted as described previously (12).

In vivo analysis of muscle function. Locomotor activity, grip force, and wire hang tests were performed essentially as described previously (15, 47).

FIG. 1. Generation of $\text{VACHT}^{\text{del/del}}$ mice. (A) Generation of $\text{VACHT}^{\text{del}}$ mice using the Cre-LoxP system. Boxes represent the different exons of ChAT or VACHT. Open boxes represent the ORF of VACHT and ChAT. Note that the VACHT gene is within the first intron of ChAT. (B) Schematic representation of the VACHT gene locus, the *floxed* allele, and the *del* allele. P1, P2, P3, and P4 indicate the positions of PCR primers used for genotyping. (C) Sequence analysis of the 329-bp fragment amplified with primers P2 and P4. Restriction sites and LoxP sequences are indicated. (D) VACHT mutant mice ($\text{VACHT}^{\text{del/del}}$) died rapidly after birth in cyanosis (not shown). Embryos from E18.5 exhibited flaccid limbs and kyphosis (hunchback). (E) Southern blot analysis confirmed the presence of the *del* allele in VACHT mutant mice. (F) Genotype of VACHT mutant mice by PCR.

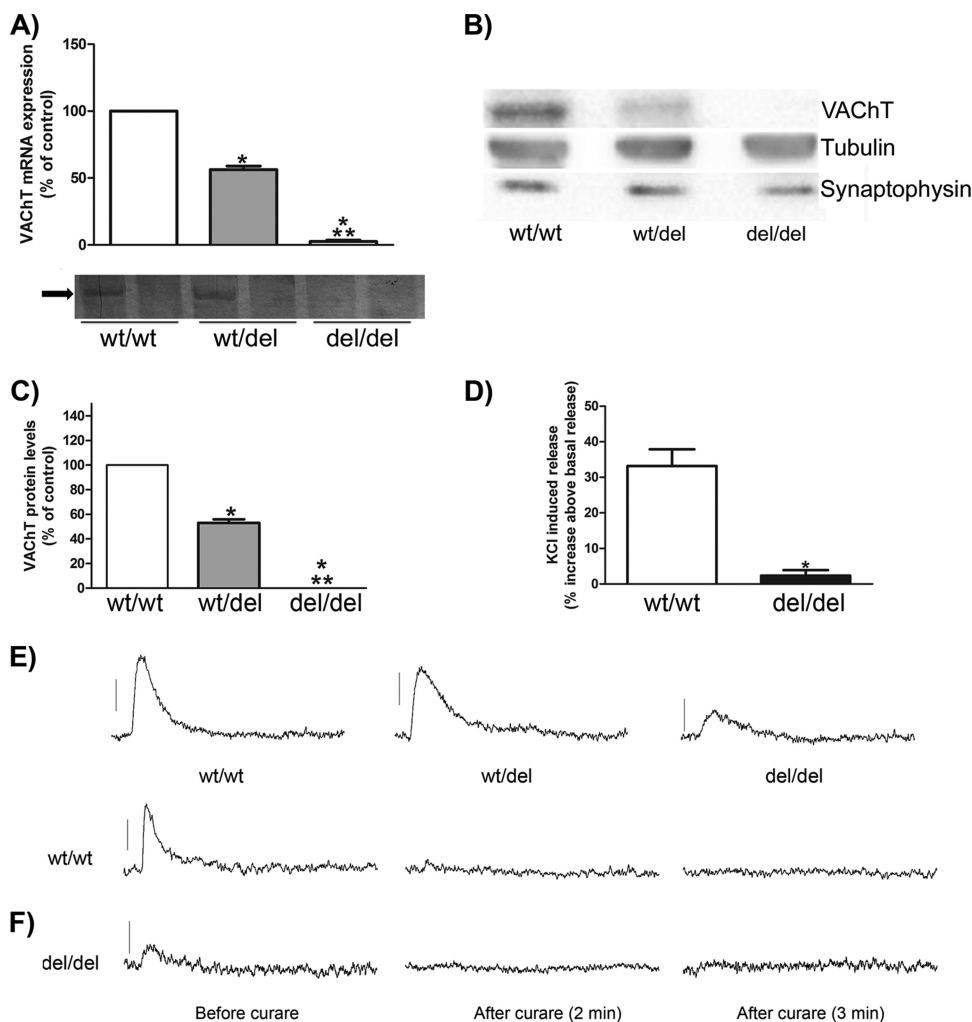


FIG. 2. VAcHT expression and ACh release in VAcHT^{del/del} E18.5 mice. (A) Quantitative analysis of VAcHT mRNA levels by qPCR. PCR products were run in a polyacrylamide gel. *, statistically different from wt; **, statistically different from wt/del {one-way ANOVA with Bonferroni post hoc [$F(2,6 = 920)$]; $P < 0.0001$; $n = 4$ }. Lanes labeled with a – show the respective negative control without the sample. (B) Western blot analysis of VAcHT, synaptophysin, and tubulin in spinal cord extracts. (C) Average values for the amount of VAcHT from densitometric analyses of several Western blots. Tubulin immunoreactivity was used to normalize protein loading. Data are presented as percentages of VAcHT^{wt/wt} levels. *, statistically different from wt; **, statistically different from wt/del {one-way ANOVA with Bonferroni post hoc [$F(2,9 = 927.9)$]; $P < 0.0001$; $n = 4$ }. (D) Effects of KCl-induced depolarization on [³H]ACh release from synaptosomes. *, statistically different from wt/wt ($P < 0.05$ by t test). (E) MEPPs from the NMJ. MEPPs recorded in VAcHT^{wt/del} muscle show no significant change in amplitude compared to VAcHT^{wt/wt} mice. VAcHT-null mice showed the existence of scarce MEPPs with decreased amplitude compared to VAcHT^{wt/wt} and VAcHT^{wt/del} mice. (F) *d*-Tubocurarine abrogated MEPPs in both VAcHT^{wt/wt} and VAcHT^{del/del} mice.

RESULTS

Generation of mice null for VAcHT. We have generated mice in which the VAcHT ORF was deleted using Cre-Lox technology (Fig. 1A and B). The deletion of the VAcHT ORF was confirmed by DNA sequencing (Fig. 1C), and we named the VAcHT-deleted allele VAcHT^{del}. The posture of VAcHT^{del/del} mice at E18.5 resembles that of ChAT-null mice, with flaccid limbs and signs of slight kyphosis (Fig. 1D). VAcHT^{del/del} mice die rapidly in cyanosis within 2 to 5 min after birth. Southern analysis (Fig. 1E) and PCR genotyping (Fig. 1F) confirmed the presence of the *del* allele in heterozygous and homozygous VAcHT mutant mice. These mice are a novel mutant line distinct from the one that we have previously described and that presents close to 70% and 45% reductions

in VAcHT expression (VAcHT KD^{HOM} and VAcHT KD^{HET}, respectively). Contrary to the mouse line reported here (VAcHT^{del/del}), the VAcHT KD lines survive to adulthood (47).

To confirm that the genetic manipulation that putatively deleted the VAcHT ORF indeed suppresses VAcHT mRNA expression, we used qPCR and E18.5 embryos (Fig. 2A). VAcHT^{wt/del} mouse brain presented a 50% decrease in the VAcHT mRNA level compared to VAcHT^{wt/wt} littermate controls. No VAcHT mRNA was detected in VAcHT^{del/del} mouse brain. The reverse transcription-PCR amplicons were also separated by electrophoresis in a polyacrylamide gel. VAcHT^{del/del} mice generated no DNA fragment corresponding to VAcHT (Fig. 2A, inset gel). VAcHT^{wt/del} mice exhibited

a 50% decrease and VACHT^{del/del} mice exhibited a 100% decrease in VACHT protein levels assayed by Western blotting of spinal cord extracts (Fig. 2B and C). The amount of synaptophysin, a protein present in synaptic vesicles, was unchanged in the spinal cord of VACHT^{del/del} mice (Fig. 2B).

To investigate the importance of VACHT for the evoked secretion of ACh, we prepared crude synaptosomes from the forebrain of E18.5 wt and homozygous mutant mice. We labeled ACh in these synaptosomes with the precursor [³H]choline and monitored the release of labeled neurotransmitter as previously described (2, 26, 27, 32). VACHT^{del/del} mice are capable of producing ACh (see Fig. 5). KCl depolarization was able to increase the release of [³H]ACh in synaptosomes obtained from wt mice but not from VACHT^{del/del} mice (Fig. 2D). Therefore, this experiment indicates that in the absence of VACHT, depolarization-evoked ACh release is hindered.

In order to analyze ACh secretion under nondepolarizing conditions, we performed electrophysiological analysis of the nerve-muscle diaphragm preparation. Figure 2E shows MEPPs recorded from NMJs of VACHT^{wt/wt}, VACHT^{wt/del}, and VACHT^{del/del} E18.5 mice. VACHT^{wt/del} mice presented no change in the amplitude of MEPPs compared to control mice (0.99 ± 0.09 mV for wt/wt and 0.92 ± 0.09 for wt/del for 31 MEPPs in three and four mice, respectively). Surprisingly, we could detect small-amplitude MEPPs in the NMJ from E18.5 embryos of VACHT^{del/del} mice (Fig. 2E). These experiments were difficult to perform, as the frequency of MEPPs in VACHT^{del/del} mice was noticeably low compared to that of VACHT^{wt/wt} embryos ($\text{del/del} = 0.0072 \pm 0.0009$ Hz [11 MEPPs obtained from four fibers from two mice]; wt/wt = 0.0308 ± 0.002 Hz [three fibers from three mice]; wt/del = 0.0364 ± 0.008 Hz [six fibers from four mice]). MEPPs from VACHT^{del/del} mice were of smaller amplitude (0.54 ± 0.07 mV). However, given the overt morphological changes at the NMJs from E18.5 VACHT^{del/del} mice (see Fig. 6, 7, and 8), both pre- and postsynaptic contributions to these changes are likely. Treatment of NMJs from control littermates and homozygous VACHT mutants with *d*-tubocurarine (5 μ M) abolished miniature detection, indicating that the MEPPs were likely recorded due to the activation of nAChR (Fig. 2F). In agreement with the fact that VACHT^{wt/del} mice presented no alteration in MEPPs at the NMJ, adult VACHT^{wt/del} mice presented no overt neuromuscular dysfunction that could be detected in a test of fatigue or grip force (Fig. 3A and B). In addition, spontaneous locomotor activity was unchanged in VACHT^{wt/del} mice (Fig. 3C).

We considered whether ACh uses another type of transporter to load synaptic vesicles in the absence of VACHT. One candidate is CHT1, which has been found to reside predominantly in synaptic vesicles by us (15, 50–52) and others (22, 36). Like other secondary active transporters for aqueous solutes, CHT1 probably functions bidirectionally (33). “Reverse transport” by CHT1 would be required to mediate ACh uptake by synaptic vesicles. We tested the possibility that CHT1 transports ACh in addition to choline by using a cell line expressing recombinant CHT1. We were not able to do the test in nerve terminals per se, as the pharmacological blockade of CHT1 would decrease ACh synthesis and potentially produce effects on small MEPPs not due to the inhibition of vesicular CHT1. To untangle the multiple possible roles of CHT1, we used a

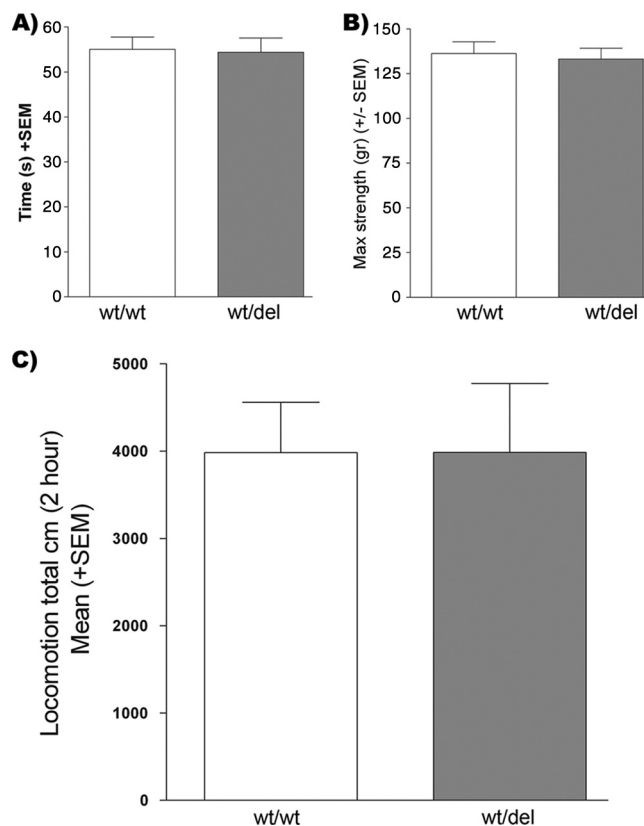


FIG. 3. Neuromuscular function in VACHT^{wt/del} mice. (A) Grip force measured for VACHT^{wt/wt} and VACHT^{wt/del} mice. There is no significant difference between the two genotypes. (B) Time spent hanging upside down from a wire netting for VACHT^{wt/wt} and VACHT^{wt/del} mice. No significant difference was observed. (C) Spontaneous locomotor activity is not changed between the genotypes.

mutant form of CHT1 (L531A) that does not undergo endocytosis, and which remains predominantly on the cell surface, to transfect HEK293 cells. The strategy is expected to maximize ACh uptake by transfected cells should CHT1 be able to transport ACh (51). As expected, transfected cells took up fourfold more choline than did nontransfected cells (Fig. 4A) (51). ACh in concentrations similar to those found in the cytoplasm of cholinergic terminals (41) inhibited choline uptake, indicating a good likelihood that ACh competes with choline for binding to CHT1 (Fig. 4B). However, the transfected cells took up no more ACh than did nontransfected cells (Fig. 4C). The results demonstrate that CHT1 does not significantly transport ACh, and thus, they do not support the possibility that CHT1 mediates the uptake of ACh by synaptic vesicles.

The results leave open the possibility that a passive transport system similar to that described previously for isolated cholinergic vesicles of *Torpedo* is present in mammalian synaptic vesicles (8). In the right circumstances, even the passive uptake of ACh by synaptic vesicles might be sufficient to generate the small MEPPs observed here. Indeed, recent experiments by Parsons and collaborators using synapse-like microvesicles from rat PC12 cells found that intact vesicles loaded with ACh lose their neurotransmitter content even when a high-affinity analog of vesamicol completely blocks VACHT. The result demonstrates an ACh leakage

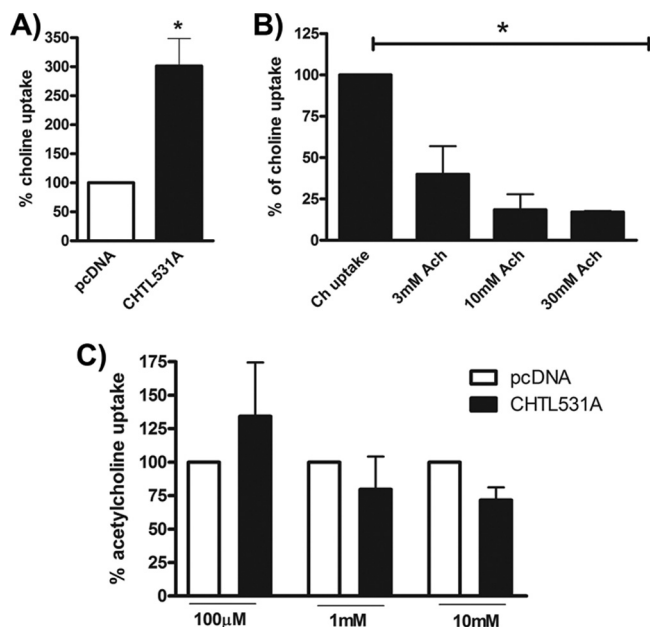


FIG. 4. (A) Choline uptake in HEK293 cells transiently transfected with empty vector (pcDNA3.1) or L531A CHT1 cDNAs. The data represent the means \pm SEM of data from five independent experiments (in duplicates) and are normalized to data for cells expressing empty vector (pcDNA3.1). *, significant difference ($P < 0.05$ by t test). (B) ACh competition assay using HEK293 cells transiently transfected with empty vector (pcDNA3.1) or L531A CHT1 cDNAs. The data represent the means \pm SEM of data from four independent experiments and are normalized to data for cells expressing the empty vector (pcDNA3.1). *, significantly different from control uptake. (C) ACh uptake in HEK293 cells transiently transfected with empty vector (pcDNA3.1) or L531A CHT1 cDNAs. The data represent the means \pm SEM of data from three independent experiments and are normalized to data for cells expressing the empty vector (pcDNA3.1).

mechanism in synapse-like microvesicles that might be bidirectional (S. M. Parsons, personal communication).

However, in order for the passive uptake of ACh by synaptic vesicles to be possible in VACHT^{del/del} mice, cytoplasmic stores of ACh must be maintained. In the absence of vesicular storage, many neurotransmitters are degraded (62), but in *C. elegans*, the mutational inactivation of VACHT leads to an increase in the ACh content of the worm (29). Therefore, we measured the amount of intracellular ACh in the brains of mutant mice. In E18.5 embryos, the amount in VACHT^{del/del} mice was more than fivefold greater than that in VACHT^{wt/wt} mice (Fig. 5A). There was also a clear tendency for the level of ACh in the brain of VACHT^{wt/del} embryos to be increased compared to that of control wt mice (Fig. 5A). In adult VACHT^{wt/del} mice, the ACh content was significantly increased compared to that of control wt mice (Fig. 5B). Because vesicles in VACHT^{del/del} mice are likely depleted of ACh, the concentration increase for ACh in the cytoplasm of cholinergic terminals is probably greater than what the bulk analysis indicates. Hence, an increased concentration of cytoplasmic ACh in VACHT^{del/del} mice might support the passive uptake of ACh into synaptic vesicles and produce small MEPPs.

Why is there so much more ACh in VACHT^{del/del} mice? One possible explanation is increases in the amounts of

either ChAT or CHT1, which are involved in the synthesis of ACh. To test for this possibility, we performed qPCR analysis of E18.5 embryos. Transcript levels for ChAT were increased in a gene dosage-dependent way (Fig. 5C). VACHT^{wt/del} mice had nearly twofold-more ChAT mRNA than their control littermates, whereas VACHT^{del/del} mice had nearly fourfold more (Fig. 5C). In addition, we found that VACHT^{del/del} mice had nearly twofold-more CHT1 mRNA than control littermates, whereas VACHT^{wt/del} mice had no significant change (Fig. 5D). At the protein level, we also detected an increase in the amounts of ChAT and CHT1 in homozygous mutant animals (Fig. 5E and F). These observations suggest that increases in ChAT and CHT1 expression levels likely underlie the increase in the amount of ACh in VACHT^{del/del} mice.

Abnormal neuromuscular patterning is a major feature of NMJ developed in the absence of ACh (4, 35). In VACHT^{del/del} mice, nerve terminals have fivefold-more ACh but lack the protein responsible for the active storage of the transmitter in vesicles. Does a lack of VACHT affect NMJ development? Can the lack of VACHT be compensated by the excess intraterminal ACh in VACHT mutants? In order to answer these questions, we evaluated nerve branching, nAChR localization, and the genesis of nerve terminals by labeling the NMJ of wt, VACHT^{wt/del}, and VACHT^{del/del} mice with distinct markers. To begin, we tested whether NMJs of VACHT^{del/del} mice showed immunoreactivity for VACHT. We found no VACHT immunoreactivity, as expected (Fig. 6A); in comparison, CHT1 immunolabeling was easily detected (Fig. 6B). Interestingly, analysis of nAChR labeling using fluorescent α -bungarotoxin-Alexa Fluor 543 (BTX-543) (Fig. 6, red) suggested an altered nAChR distribution (Fig. 6A and B and higher magnification in C). Indeed, clusters of nAChR labeled with BTX-543 showed stronger labeling and a larger area in VACHT^{del/del} mice than the corresponding labeling in control and VACHT^{wt/del} mice (Fig. 6C and D) (the increase in labeling was close to 70%).

The rescue of MNs from physiologically programmed cell death that follows the blockade of neuromuscular activity during development is a well-known phenomenon (38, 39). The disturbance of ACh synthesis also affects MN apoptosis (4). In order to test if in the absence of VACHT MNs went through the normal wave of apoptosis, we counted lumbar MNs from wt and VACHT^{del/del} E18.5 embryos (Fig. 6E). Of note, there was a significant increase in the number of MNs in VACHT mutant mice compared to wt controls (36%), suggesting that VACHT-independent ACh secretion did not generate the muscle activity necessary for the programmed cell death of MNs during development. The increase in MN survival was similar to but somewhat less severe than that observed for ChAT-null mice (Fig. 6E) (51% increase in the number of neurons compared to wt controls).

To examine if the enhanced nAChR labeling and enhanced MN numbers are accompanied by an increase in the number of nerve terminals in VACHT^{del/del} mice, we quantified the number of CHT1-positive nerve terminals. Immunoreactivity for CHT1 (Fig. 7A) was increased at the NMJ, confirming the biochemical data shown in Fig. 5D and F. We also quantified the number of CHT1-positive nerve terminals, and we detected a significant increase in the number of CHT1-positive nerve

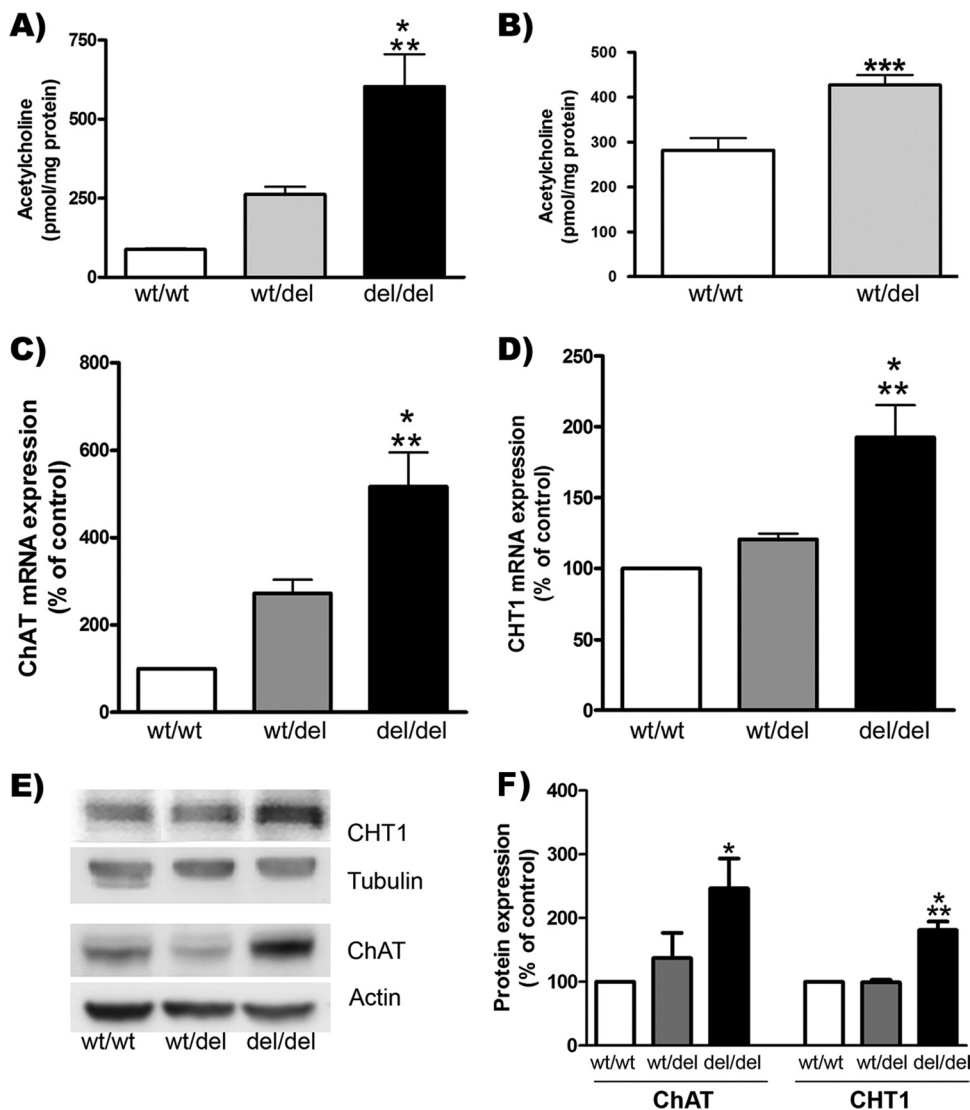


FIG. 5. Neurochemical alterations in VACHT^{del/del} mice. (A) Intracellular ACh contents in brains of VACHT mutant mouse embryos. Data are means \pm SEM (three to five mice). An asterisk indicates a statistically significant difference by one-way ANOVA with Bonferroni post hoc test [$F(2,10) = 12.72$]. (B) Intracellular ACh content in brains from adult VACHT^{wt/wt} and VACHT^{wt/del} mice ($n = 4$ to 6 brains) (***, $P < 0.001$). (C) ChAT mRNA levels detected by qPCR from E18.5 mouse brains [$F(2,9) = 18.28$] ($n = 4$). (D) CHT1 mRNA levels detected by qPCR from E18.5 mouse brains. *, statistically different from VACHT^{wt/wt} mice; **, statistically different from VACHT^{wt/del} mice [$F(2,11) = 12.52$] ($n = 5$). (E) ChAT and CHT1 protein expression in E18.5 spinal cords. (F) Quantification of protein expression (three to four animals) ($P < 0.05$) [CHT1 $F(2,6) = 35.21$; ChAT $F(2,15) = 4.599$]. *, statistically different from wt/wt; **, statistically different from wt/del.

endings in VACHT-null mutants (Fig. 7B). To further test if the nerve endings in the diaphragm of VACHT^{del/del} mice were able to undergo exocytosis-endocytosis, we used a form of the activity-dependent dye FM1-43, FM1-43fx, that can be used for protocols requiring tissues to undergo fixation. Preparations to be stained with FMI-43fx underwent KCl-mediated depolarization as described previously (47, 53) and were then washed and fixed prior to the quantification of fluorescently labeled nerve terminals. The results show that synaptic vesicles in VACHT^{del/del} mice undergo exocytosis-endocytosis. Moreover, muscles from homozygous mutants have an increased density of stained nerve terminals compared to control wt mice (40% increase) (Fig. 7C and D). Figure 7E shows an example of terminals labeled with FM dye, and Fig. 7F indicates that in

addition to an increase in the number of terminals, the area of the individual terminals labeled with FM1-43 from VACHT^{del/del} mice is also increased compared to that from VACHT^{wt/wt} mice ($P = 0.0018$). The increase in the number of nerve terminals appears to be a consequence of the complete loss of VACHT, as VACHT KD^{HOM} mice that preserve 30% of normal levels of the transporter show no such increase (48; data not shown). VACHT KD^{HOM} mice also did not show an increase in the number of MNs, suggesting that reducing VACHT levels by up to 70% can still support enough release of neurotransmitter during development to maintain the program of MN cell death (data not shown).

To further examine axonal targeting at the NMJ in the absence of VACHT, we labeled diaphragms from wt,

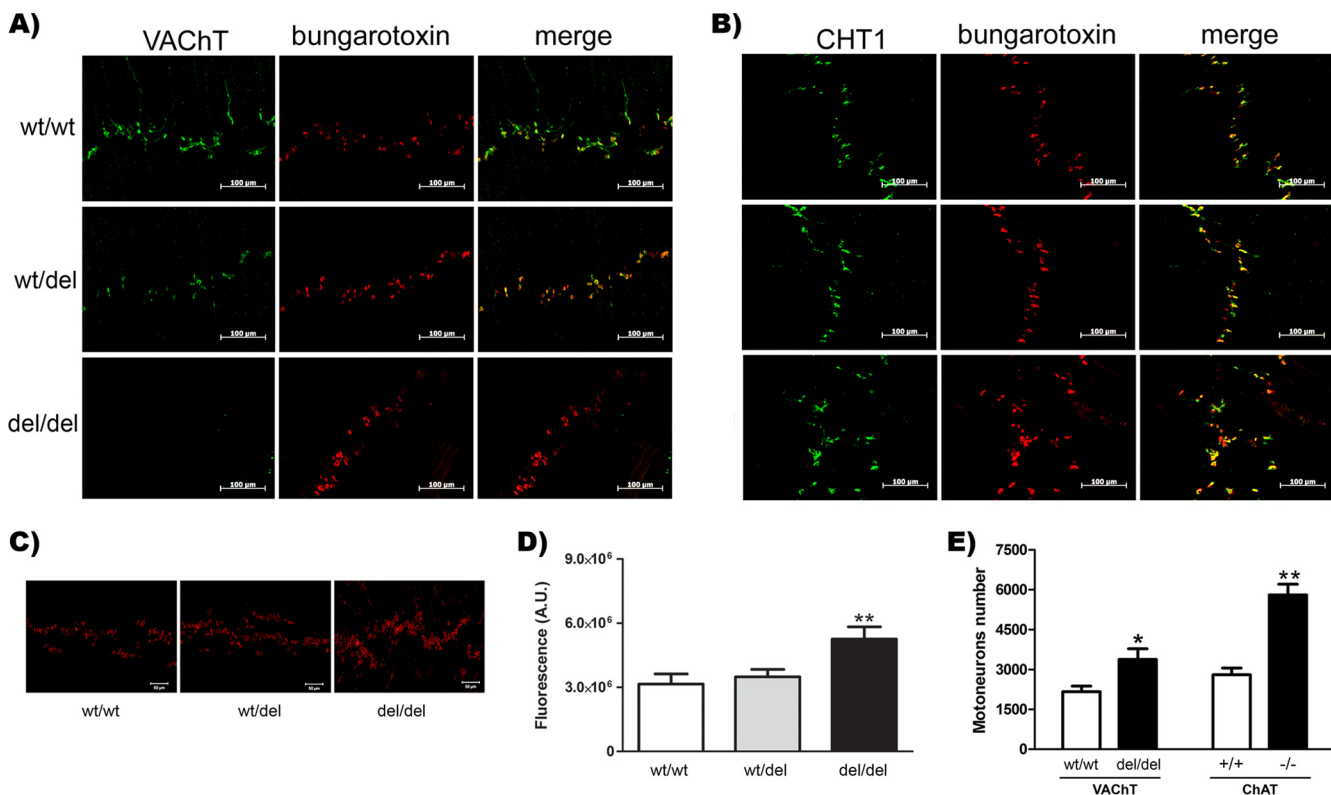


FIG. 6. Alterations in MN number and in NMJ morphology in VACHT^{del/del} E18.5 mice. (A) VACHT immunoreactivity was easily detected in presynaptic termini of VACHT^{wt/wt} and VACHT^{wt/del} diaphragms but was absent in VACHT^{del/del} mice. (B) CHT1 immunoreactivity was detected in all genotypes, although VACHT^{del/del} mice showed an altered distribution of nerve endings (see below and Fig. 5). (C) Abnormal distribution of nAChR in VACHT^{del/del} NMJs. Images show that nAChRs from VACHT^{del/del} mice present stronger labeling and are distributed over a broader region than those from wt and VACHT^{wt/del} mice. (D) Quantification of nAChR fluorescence. Four independent experiments were performed, and the results are expressed as means \pm SEM. An asterisk indicates a statistically significant difference (one-way ANOVA with Bonferroni post hoc) [$F(2,20) = 5.632$]. A.U., arbitrary units. (E) The number of lumbar MNs was significantly increased in VACHT and ChAT-null mice. Clear bars, wt mice; dark bars, homozygous mutant mice.

VACHT^{wt/del}, and VACHT^{del/del} mice with an anti-neurofilament antibody (Fig. 8, red) and nAChR with BTX-Alexa Fluor 488 (Fig. 8, green). These experiments show that there is no difference in axonal branching between wt and VACHT^{wt/del} mice. Axon branches from the nerves labeled with the anti-neurofilament antibody were of the characteristic size and generally contacted a cluster of nAChR (Fig. 8). In contrast, VACHT^{del/del} mice had an increase in axonal sprouting and branching that contacted improperly arranged nAChR clusters (Fig. 8). The morphology of the NMJ from VACHT^{del/del} mice was remarkably similar to that reported for ChAT-deficient mice. In fact, in hematoxylin- and eosin-stained muscles, we note that sheets of condensed parallel fusiform nuclei with abundant myofibrillar tissue could be easily discerned in VACHT^{wt/wt} and VACHT^{wt/del} mice (Fig. 9A and B). In contrast, myofibrillar tissue was replaced with fragmented myofibrils in VACHT^{del/del} mice (Fig. 9C). In some cases, there was a complete loss of normal architecture in mutant muscles, and degenerated myofibrils were replaced with fibrotic and fatty tissue (Fig. 6C). Relative to the controls, skeletal muscles from VACHT^{del/del} mice showed marked atrophy. These findings suggest that in the absence of VACHT, despite the nerve terminals having increased ACh contents, the outcome for NMJ development was as severe as the lack of ACh synthesis.

DISCUSSION

The present work addresses the role of VACHT in sustaining the release of ACh. We found that VACHT is fundamental for ACh release in the brain and the NMJ. Moreover, in the absence of the vesicular transport of ACh, there are profound effects on axons, terminal numbers, and synaptic and muscle morphology at the NMJ. Indeed, VACHT-null mice, despite presenting fivefold-more ACh than control mice, recapitulate the NMJ phenotype found in mice that cannot synthesize ACh due to a lack of ChAT. These observations bear important consequences for understanding how developing synapses function and the mechanisms by which transmitter secretion during development regulates synaptic targeting.

VACHT knockout mice do not survive postnatally. The pharmacological inhibition of VACHT causes paralysis and death compatible with an NMJ blockade (5), indicating that interference with VACHT might be lethal. Given the observations that ChAT-null mice have abnormal NMJ development (4, 35), the question arises of whether it is just the presence of ACh that is required or if the VACHT-mediated storage of ACh during development is also important. Previous experiments with munc18-1 null mice, which have no regulated secretion of a neurotransmitter, also suggested that NMJ development is reg-

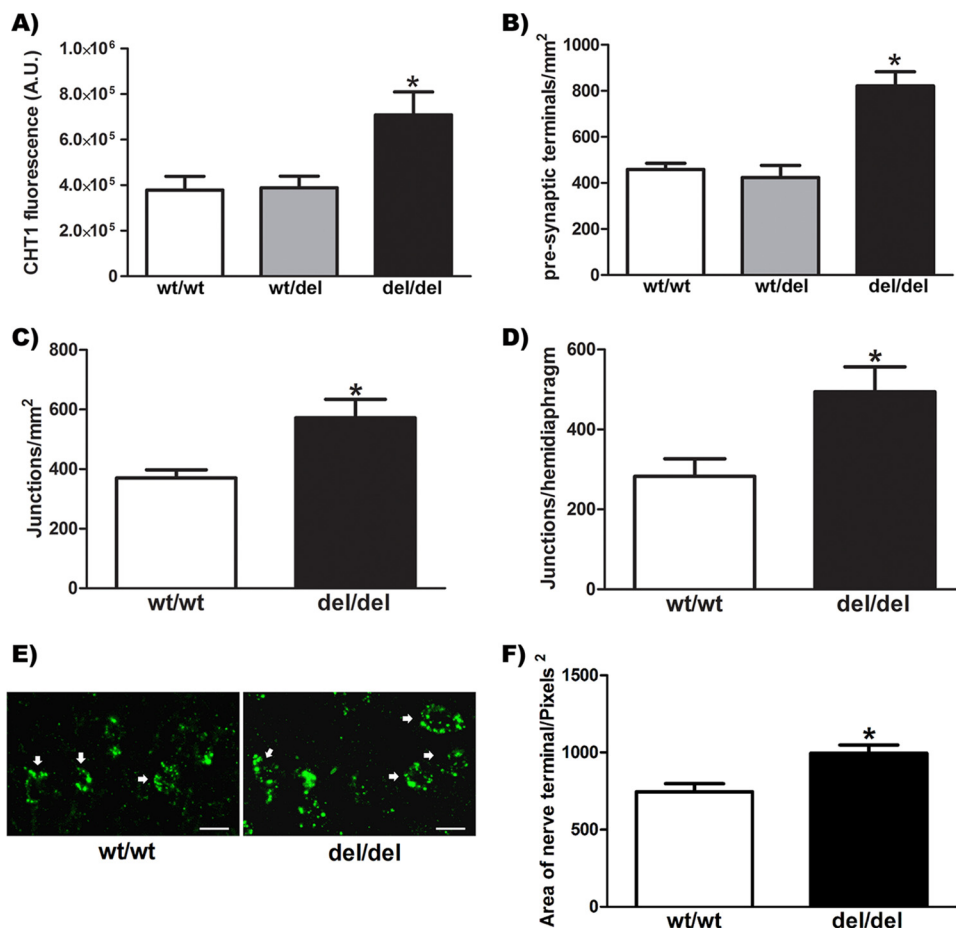


FIG. 7. Synaptic alteration in VACHT^{del/del} E18.5 mice. (A) Quantification of CHT1 fluorescence (arbitrary units [A.U.]) in nerve terminals. An asterisk indicates a statistically significant difference (one-way ANOVA with Bonferroni post hoc test) [$F(2,20) = 5.632$]. (B) Density of nerve terminals immunolabeled for CHT1 in hemidiaphragms from VACHT^{wt/wt}, VACHT^{wt/del}, and VACHT^{del/del} mice. *, statistically different by ANOVA with Bonferroni post hoc test [$F(2,17) = 18.43$]. (C) Density of nerve terminals stained with FM1-43fx in hemidiaphragms of VACHT^{wt/wt} and VACHT^{del/del} mice (*, $P = 0.0218$ for VACHT^{wt/wt} versus VACHT^{del/del} mice by unpaired t test; $n = 6$). (D) Number of nerve terminals stained with FM1-43fx per hemidiaphragm (*, $P = 0.0260$ for VACHT^{wt/wt} versus VACHT^{del/del} mice by unpaired t test; $n = 6$). (E) Representative images of NMJs stained with FM1-43fx in hemidiaphragms of VACHT^{wt/wt} and VACHT^{del/del} mice (scale bar, 10 μ m). (F) Average area of single nerve terminals in mouse hemidiaphragms stained with FM1-43fx (*, $P = 0.0018$ for VACHT^{wt/wt} versus VACHT^{del/del} mice by unpaired t test). At least 30 end plates were analyzed for each genotype.

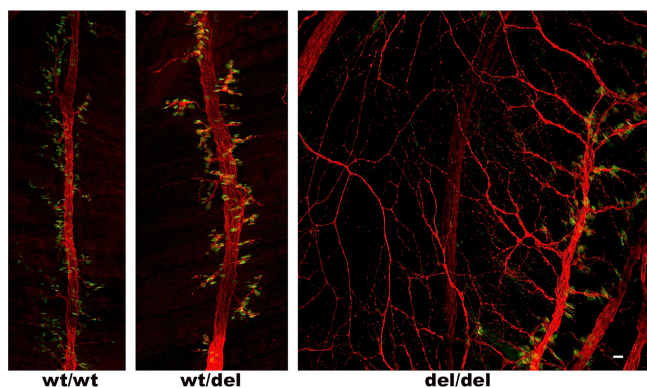


FIG. 8. Altered morphology at the NMJ of VACHT^{del/del} E18.5 mice. Whole diaphragms were stained with anti-neurofilament antibody (red), and nAChRs were labeled with α -bungarotoxin (green). Confocal stacks were obtained, and maximal projections are shown in the images. The image is representative of three experiments. Note the large increase in axonal sprouting in VACHT-null mice.

ulated by synaptic vesicle exocytosis, although for these mutants, it has not been established whether ACh synthesis and storage are affected (28). A number of previously reported studies suggested that distinct pathways of ACh secretion might exist at cholinergic synapses (56, 60, 61, 64). Moreover, vesamicol-independent ACh release, presumably from synaptic vesicles, can be detected in response to pharmacological treatments (2, 7, 10, 11, 46). Hence, if VACHT-independent mechanisms of ACh release have functional significance, they might partially compensate for the lack of the transporter in at least some of its physiological roles.

Interestingly, experiments with an independent mouse line, VACHT KD^{HET} mice, that have close to a 40% reduction in VACHT expression levels showed that a moderate reduction in the level of VACHT causes no neuromuscular phenotype and only small changes in neuromuscular neurotransmission (47). Similar results were obtained with VACHT^{wt/del} mice in the present report, suggesting an important safety mechanism at

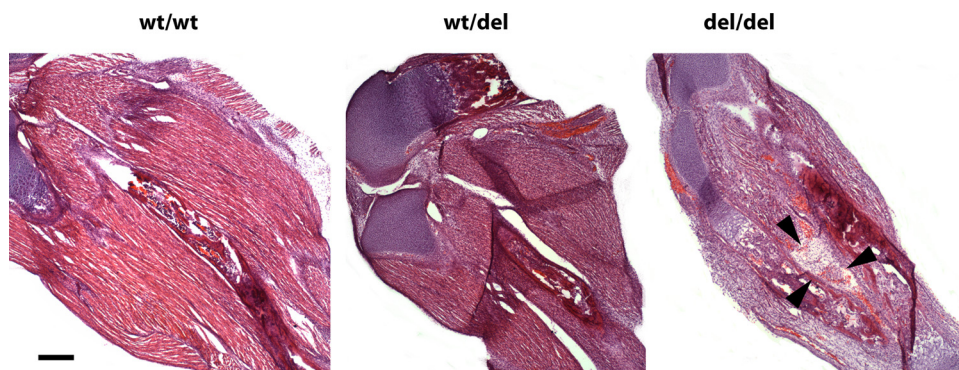


FIG. 9. Muscle morphology of E18.5 embryos from $VACHT^{wt/wt}$, $VACHT^{wt/del}$, and $VACHT^{del/del}$ genotypes. Skeletal muscles (gastrocnemius) were stained with hematoxylin and eosin. Black arrows indicate a loss of normal myofibrillar architecture. Bar, 250 μ m.

the NMJ that allows decreased VACHT expression to be compensated. However, $VACHT^{KD^{HOM}}$ mice, with close to a 70% decrease in VACHT protein levels, do show alterations in neuromuscular neurotransmission and motor function (47). It should be noted, however, that synapses in the central nervous system are more sensitive to reductions in VACHT expression, and both $VACHT^{KD^{HET}}$ mice (47) and $VACHT^{wt/del}$ mice (our unpublished observations) present selective cognitive deficits in object recognition memory.

Despite this substantial compensation, the rapid postnatal death of $VACHT^{del/del}$ mice argues that the active storage of ACh by this transporter is critical at the NMJ, as the mice succumb to respiratory failure. In agreement with this conclusion, synaptosomes from $VACHT^{del/del}$ mice do not release newly synthesized ACh in response to depolarization. Lethal mutants of VACHT have also been generated in *Drosophila melanogaster*. These mutants are apparently expressed as well as wt alleles, but they have affected VACHT transport activity (31). Lethal alleles of *unc-17* in *C. elegans* have also been identified, indicating that VACHT is critical for survival in several organisms (1).

VACHT regulates cholinergic synaptic development. Whereas it is clear that ACh storage by VACHT is important for motor function, it is possible that during development, other mechanisms of ACh release, which are independent of this transporter, might become relevant. In nerve-muscle cocultures, a nonquantal release of ACh can be detected in developing growth cones (56). Moreover, compelling genetic evidence from *Drosophila* suggests that the correct axonal targeting of photoreceptors depends on ACh synthesis but not on the expression of VACHT or on synaptic vesicle exocytosis (64). Hence, at least in *Drosophila*, a VACHT-independent mechanism of secretion appears to be important during development. In the light of these findings, we examined whether neuromuscular development in mouse embryos depends on the VACHT-mediated storage of ACh.

Surprisingly, recordings from the diaphragm of $VACHT^{del/del}$ mice revealed small MEPPs, raising the possibility that they arise from small quanta of ACh. Experiments with curare confirmed that these MEPPs were due to the activation of nAChR. We tested the possibility that CHT1 can transport ACh, which might have explained the transport of ACh in vesicles lacking VACHT. A functional mutant of CHT1 retained on the cytoplasmic mem-

brane was expressed in HEK293 cells, and the transfected cells were tested for an enhanced uptake of ACh. None was detected. Moreover, at the low internal pH of synaptic vesicles, CHT1 probably cannot transport substrates (30). We cannot completely eliminate the possibility that ATP or another vesicular constituent is released and activates nicotinic receptors, although the blockade of the small MEPP by curare indicates that ACh itself is the agent.

Early work on vesicles isolated from *Torpedo* electric organs identified a passive accumulation of ACh that could account for up to one-third of the total transport (8). More recent unpublished data indicate that isolated synapse-like microvesicles loaded with radiolabeled ACh lose their neurotransmitter by a VACHT-independent pathway (S. M. Parsons, personal communication). The experiments suggest that ACh can permeate vesicular membranes in the absence of active transport. Given that levels of intracellular ACh are increased fivefold in $VACHT^{del/del}$ mice, creating a very large gradient between the cytoplasm and the lumen of synaptic vesicles, we favor the possibility that the small MEPPs detected in $VACHT^{del/del}$ NMJs result from the passive entry of ACh into vesicles. In fact, vesicles from $VACHT^{del/del}$ NMJs can be loaded with FM1-43, confirming that "empty" vesicles undergo exocytosis-endocytosis (9, 40). However, a stimulated release of newly synthesized ACh from brain synaptosomes obtained from $VACHT^{del/del}$ mice did not occur, indicating that this putative passive transport is much less efficient and may require much more time than the active VACHT-mediated transport.

It seems unlikely that the VACHT-independent secretion of ACh, as recently detected for *Drosophila* (64), has a major role during the development of the mammalian NMJ based on our assessment of muscle morphology, axonal patterning, MN survival, and synaptogenesis in $VACHT^{del/del}$ mice. It is well established that the survival of MN, as well as proper axonal and synaptic targeting, depends on effective competition for neurotrophic support that can be modulated by muscle activity during embryogenesis. ACh has been recognized to act as a signal that induces proper axonal branching, nerve terminal size, and number and maturation of synapses. It likely generates muscle activity leading to the secretion of neurotrophic factors during embryonic development (4, 35). The programmed cell death of MNs is also regulated by ACh, and

ChAT-null mice have an increased number of MNs (4, 6, 35). These results are consistent with the well-known phenomenon of increased survival of MNs after a pharmacological blockade of muscle nAChR during development (38, 39, 42). Our observation that VACHT^{del/del} mice, despite having a fivefold increase in tissue ACh levels, have alterations in neuromuscular development similar to that seen for ChAT-deficient mice strongly suggests that passive uptake by vesicles or even a leakage of ACh from nerve terminals cannot compensate for the lack of VACHT. In fact, the increase in ChAT, CHT1, and ACh contents should conspire to facilitate ACh leakage in VACHT^{del/del} mice but apparently to no avail. It is curious, however, that the VACHT-independent ACh secretion described previously for *Drosophila* (64) does not operate in the mammalian NMJ. The difference between mice and flies may relate to the fact that ACh in *Drosophila* photoreceptors is not the chemical transmitter of these synapses as it is for the mammalian NMJ (64); rather, ACh in the fly photoreceptor seems to function as a developmental cue, whereas histamine is the actual neurotransmitter.

Cytoplasmic ACh in the absence of VACHT. We also find that the removal of the VACHT gene, which is embedded in the first intron of the ChAT gene, causes several neurochemical alterations in cholinergic synapses. The large increase in the ACh content is opposite from what happens in mice null for vesicular monoamine transporter 2, as they have a decrease in intracellular monoamine contents (62). *C. elegans* carrying a blocking mutation of VACHT also has an increase in ACh contents (29, 65).

The increase in the ACh content in mutant mice is likely due to increased levels of expression of ChAT and CHT1. The change in ChAT expression may be related to a compensatory mechanism due to the lack of ACh release, but it might also arise from the physical removal of a large fragment of the ChAT gene, which includes a large part of the first intron (after the R exon), the N exon, and part of the second intron. This deletion physically places the M promoter of ChAT close to the promoter for VACHT and potentially could increase the level of expression of ChAT mRNAs. However, given the fact that the CHT1 expression level is also increased, it is possible that the lack of evoked ACh release triggers signals that up-regulate the ACh synthesis machinery. Moreover, the increase in the number of MNs can also contribute to the increased levels of CHT1 and ChAT in the spinal cord. Given that individual synaptic terminals at the NMJ show increased CHT1 expression levels by immunofluorescence, we favor the possibility that both increased expression levels and the increased number of neurons contribute to the higher levels of CHT1 and ChAT. It remains to be determined if cholinergic neurons in the brain present similar changes in morphology and sprouting.

Our data suggest that changes in levels of expression of ChAT and CHT1 "in vivo" can effectively increase the ACh content in cholinergic terminals. Moreover, it seems that the excess ACh in the cytoplasm can be accumulated without degradation, suggesting that "in vivo," this excessive amount of ACh does not impair ACh synthesis. These results agree with data from previously reported experiments performed in the presence of the VACHT inhibitor vesamicol, which, in the superior cervical ganglion, impairs ACh release and allows an accumulation of cytoplasmic ACh (13). These data suggest that ACh synthesis is not regulated

by mass action, as previously proposed by a number of investigators (25, 57, 58), because in the absence of ACh release, the transmitter continues to accumulate.

Previous results indicated that both the exocytosis-endocytosis of synaptic vesicles and the quantal release of the neurotransmitter occur in developing axons (24, 34). Our experiments indicate that VACHT regulates a key step for physiologically relevant neurotransmission during the development of the NMJ.

ACKNOWLEDGMENT

We are indebted to Scott Zeitlin (Department of Neuroscience, University of Virginia School of Medicine) for the gift of Cre mice, Stanley Parsons (UCSB) for sharing unpublished data and for excellent suggestions for editing the manuscript, and Brian Collier (McGill University) for comments on the manuscript.

Research in our laboratory is supported by NIH-Fogarty grant R21 TW007800-02 (M.A.M.P., I.I., V.F.P., and M.G.C.), NIH grant RO1 NS53527 (R.W.O.), CIHR (MOP-89919 [V.F.P., R.J.R., and M.A.M.P.]), PRONEX-Fapemig (M.A.M.P. and V.F.P.), FINEP (M.A.M.P.), CNPq (Aging and Mental Health Programs [M.A.M.P., V.F.P., I.I., and M.C.]), FAPEMIG (V.F.P.), and Instituto do Milenio Toxins/MCT (M.V.G., M.A.M.P., and V.F.P.). C.M.-S. and C.M. received postdoctoral fellowships from DFAIT-Canada (Department of Foreign Affairs and International Trade Postdoctoral Fellowship Program). B.M.D.C., X.D.J., and R.L.F. received predoctoral student fellowships from CAPES and CNPq (Brazil).

M.G.C., M.A.M.P., V.F.P., I.I., C.M.-S., and B.M.D.C. have deposited a patent to cover the use of VACHT mutant mice in drug discovery.

REFERENCES

- Alfonso, A., K. Grundahl, J. S. Duerr, H. P. Han, and J. B. Rand. 1993. The *Caenorhabditis elegans* unc-17 gene: a putative vesicular acetylcholine transporter. *Science* **261**:617-619.
- Barbosa, J., Jr., A. D. Clarizia, M. V. Gomez, M. A. Romano-Silva, V. F. Prado, and M. A. Prado. 1997. Effect of protein kinase C activation on the release of [³H]acetylcholine in the presence of vesamicol. *J. Neurochem.* **69**:2608-2611.
- Bradford, M. M. 1976. A rapid and sensitive method for the quantitation of microgram quantities of protein utilizing the principle of protein-dye binding. *Anal. Biochem.* **72**:248-254.
- Brandon, E. P., W. Lin, K. A. D'Amour, D. P. Pizzo, B. Dominguez, Y. Sugiura, S. Thode, C. P. Ko, L. J. Thal, F. H. Gage, and K. F. Lee. 2003. Aberrant patterning of neuromuscular synapses in choline acetyltransferase-deficient mice. *J. Neurosci.* **23**:539-549.
- Brittain, R. T., G. P. Levy, and M. B. Tyers. 1969. The neuromuscular blocking action of 2-(4-phenylpiperidino)cyclohexanol (AH 5183). *Eur. J. Pharmacol.* **8**:93-99.
- Buss, R. R., T. W. Gould, J. Ma, S. Vinsant, D. Prevet, A. Winseck, K. A. Toops, J. A. Hammarback, T. L. Smith, and R. W. Oppenheim. 2006. Neuromuscular development in the absence of programmed cell death: phenotypic alteration of motoneurons and muscle. *J. Neurosci.* **26**:13413-13427.
- Cabeza, R., and B. Collier. 1988. Acetylcholine mobilization in a sympathetic ganglion in the presence and absence of 2-(4-phenylpiperidino)cyclohexanol (AH5183). *J. Neurochem.* **50**:112-121.
- Carpenter, R. S., R. Koenigsberger, and S. M. Parsons. 1980. Passive uptake of acetylcholine and other organic cations by synaptic vesicles from Torpedo electric organ. *Biochemistry* **19**:4373-4379.
- Ceccarelli, B., and W. P. Hurlbut. 1975. The effects of prolonged repetitive stimulation in hemicholinium on the frog neuromuscular junction. *J. Physiol.* **247**:163-188.
- Clarizia, A. D., M. V. Gomez, M. A. Romano-Silva, S. M. Parsons, V. F. Prado, and M. A. Prado. 1999. Control of the binding of a vesamicol analog to the vesicular acetylcholine transporter. *Neuroreport* **10**:2783-2787.
- Clarizia, A. D., M. A. Romano-Silva, V. F. Prado, M. V. Gomez, and M. A. M. Prado. 1998. Role of protein kinase C in the release of [H-3]acetylcholine from myenteric plexus treated with vesamicol. *Neurosci. Lett.* **244**:115-117.
- Clarke, P. G., and R. W. Oppenheim. 1995. Neuron death in vertebrate development: in vitro methods. *Methods Cell Biol.* **46**:277-321.
- Collier, B., S. A. Welner, J. Ricny, and D. M. Araujo. 1986. Acetylcholine synthesis and release by a sympathetic ganglion in the presence of 2-(4-phenylpiperidino)cyclohexanol (AH5183). *J. Neurochem.* **46**:822-830.
- Dan, Y., and M. M. Poo. 1992. Quantal transmitter secretion from myocytes loaded with acetylcholine. *Nature* **359**:733-736.
- de Castro, B. M., G. S. Pereira, V. Magalhães, J. I. Rossato, X. De Jaeger, C.

- Martins-Silva, B. Leles, P. Lima, M. V. Gomez, R. R. Gainetdinov, M. G. Caron, I. Izquierdo, M. Cammarota, V. F. Prado, and M. A. Prado. 2009. Reduced expression of the vesicular acetylcholine transporter causes learning deficits in mice. *Genes Brain Behav.* **8**:23–35.
16. Dobransky, T., and R. J. Rylett. 2005. A model for dynamic regulation of choline acetyltransferase by phosphorylation. *J. Neurochem.* **95**:305–313.
 17. Dragatsis, I., and S. Zeitlin. 2000. CaMKIIalpha-Cre transgene expression and recombination patterns in the mouse brain. *Genesis* **26**:133–135.
 18. Edwards, R. H. 2007. The neurotransmitter cycle and quantal size. *Neuron* **55**:835–858.
 19. Estrella, D., K. L. Green, C. Prior, J. Dempster, R. F. Halliwell, R. S. Jacobs, S. M. Parsons, R. L. Parsons, and I. G. Marshall. 1988. A further study of the neuromuscular effects of vesamicol (AH5183) and of its enantiomer specificity. *Br. J. Pharmacol.* **93**:759–768.
 20. Falk-Vairant, J., P. Correges, L. Eder-Colli, N. Salem, E. Roulet, A. Bloc, F. Meunier, B. Lesbats, F. Loctin, M. Synguelakis, M. Israel, and Y. Dunant. 1996. Quantal acetylcholine release induced by mediatoaphore transfection. *Proc. Natl. Acad. Sci. USA* **93**:5203–5207.
 21. Ferguson, S. M., M. Bazalakova, V. Savchenko, J. C. Tapia, J. Wright, and R. D. Blakely. 2004. Lethal impairment of cholinergic neurotransmission in hemicholinium-3-sensitive choline transporter knockout mice. *Proc. Natl. Acad. Sci. USA* **101**:8762–8767.
 22. Ferguson, S. M., V. Savchenko, S. Apparsundaram, M. Zwick, J. Wright, C. J. Heilman, H. Yi, A. I. Levey, and R. D. Blakely. 2003. Vesicular localization and activity-dependent trafficking of presynaptic choline transporters. *J. Neurosci.* **23**:9697–9709.
 23. Ferguson, S. S., and M. G. Caron. 2004. Green fluorescent protein-tagged beta-arrestin translocation as a measure of G protein-coupled receptor activation. *Methods Mol. Biol.* **237**:121–126.
 24. Girod, R., S. Popov, J. Alder, J. Q. Zheng, A. Lohof, and M. M. Poo. 1995. Spontaneous quantal transmitter secretion from myocytes and fibroblasts: comparison with neuronal secretion. *J. Neurosci.* **15**:2826–2838.
 25. Glover, V. A., and L. T. Potter. 1971. Purification and properties of choline acetyltransferase from ox brain striate nuclei. *J. Neurochem.* **18**:571–580.
 26. Gomez, R. S., M. V. Gomez, and M. A. Prado. 1996. Inhibition of Na⁺, K⁺-ATPase by ouabain opens calcium channels coupled to acetylcholine release in guinea pig myenteric plexus. *J. Neurochem.* **66**:1440–1447.
 27. Gomez, R. S., M. A. Prado, F. Carazza, and M. V. Gomez. 1999. Halothane enhances exocytosis of [³H]-acetylcholine without increasing calcium influx in rat brain cortical slices. *Br. J. Pharmacol.* **127**:679–684.
 28. Heeroma, J. H., J. J. Plomp, E. W. Rouboos, and M. Verhage. 2003. Development of the mouse neuromuscular junction in the absence of regulated secretion. *Neuroscience* **120**:733–744.
 29. Hosono, R., T. Sassa, and S. Kuno. 1987. Mutations affecting acetylcholine levels in the nematode *Caenorhabditis elegans*. *J. Neurochem.* **49**:1820–1823.
 30. Iwamoto, H., R. D. Blakely, and L. J. De Felice. 2006. Na⁺, Cl⁻, and pH dependence of the human choline transporter (hCHT) in *Xenopus* oocytes: the proton inactivation hypothesis of hCHT in synaptic vesicles. *J. Neurosci.* **26**:9851–9859.
 31. Kitamoto, T., X. Xie, C. F. Wu, and P. M. Salvaterra. 2000. Isolation and characterization of mutants for the vesicular acetylcholine transporter gene in *Drosophila melanogaster*. *J. Neurobiol.* **42**:161–171.
 32. Leao, R. M., M. V. Gomez, B. Collier, and M. A. Prado. 1995. Inhibition of potassium-stimulated acetylcholine release from rat brain cortical slices by two high-affinity analogs of vesamicol. *Brain Res.* **703**:86–92.
 33. Marchbanks, R. M., S. Wonnacott, and M. A. Rubio. 1981. The effect of acetylcholine release on choline fluxes in isolated synaptic terminals. *J. Neurochem.* **36**:379–393.
 34. Matteoli, M., K. Takei, M. S. Perin, T. C. Sudhof, and P. De Camilli. 1992. Exo-endocytic recycling of synaptic vesicles in developing processes of cultured hippocampal neurons. *J. Cell Biol.* **117**:849–861.
 35. Misgeld, T., R. W. Burgess, R. M. Lewis, J. M. Cunningham, J. W. Lichtman, and J. R. Sanes. 2002. Roles of neurotransmitter in synapse formation: development of neuromuscular junctions lacking choline acetyltransferase. *Neuron* **36**:635–648.
 36. Nakata, K., T. Okuda, and H. Misawa. 2004. Ultrastructural localization of high-affinity choline transporter in the rat neuromuscular junction: enrichment on synaptic vesicles. *Synapse* **53**:53–56.
 37. Nguyen, M. L., G. D. Cox, and S. M. Parsons. 1998. Kinetic parameters for the vesicular acetylcholine transporter: two protons are exchanged for one acetylcholine. *Biochemistry* **37**:13400–13410.
 38. Oppenheim, R. W., J. Caldero, D. Cuitat, J. Esquerda, J. J. McArdle, B. M. Olivera, D. Prevette, and R. W. Teichert. 2008. The rescue of developing avian motoneurons from programmed cell death by a selective inhibitor of the fetal muscle-specific nicotinic acetylcholine receptor. *Dev. Neurobiol.* **68**:972–980.
 39. Oppenheim, R. W., D. Prevette, A. D'Costa, S. Wang, L. J. Houenou, and J. M. McIntosh. 2000. Reduction of neuromuscular activity is required for the rescue of motoneurons from naturally occurring cell death by nicotinic-blocking agents. *J. Neurosci.* **20**:6117–6124.
 40. Parsons, R. L., M. A. Calupca, L. A. Merriam, and C. Prior. 1999. Empty synaptic vesicles recycle and undergo exocytosis at vesamicol-treated motor nerve terminals. *J. Neurophysiol.* **81**:2696–2700.
 41. Parsons, S. M. 2000. Transport mechanisms in acetylcholine and monoamine storage. *FASEB J.* **14**:2423–2434.
 42. Pittman, R., and R. W. Oppenheim. 1979. Cell death of motoneurons in the chick embryo spinal cord. IV. Evidence that a functional neuromuscular interaction is involved in the regulation of naturally occurring cell death and the stabilization of synapses. *J. Comp. Neurol.* **187**:425–446.
 43. Pittman, R. H., and R. W. Oppenheim. 1978. Neuromuscular blockade increases motoneurone survival during normal cell death in the chick embryo. *Nature* **271**:364–366.
 44. Prado, M. A., T. Moraes-Santos, R. N. Freitas, M. A. Silva, and M. V. Gomez. 1990. Choline oxidase chemiluminescent assay, after removal of eserine from medium, of acetylcholine released in vitro from brain slices. *J. Neurosci. Methods* **31**:193–196.
 45. Prado, M. A. M., M. V. Gomez, and B. Collier. 1992. Mobilization of the readily releasable pool of acetylcholine from a sympathetic-ganglion by tityustoxin in the presence of vesamicol. *J. Neurochem.* **59**:544–552.
 46. Prado, M. A. M., M. V. Gomez, and B. Collier. 1993. Mobilization of a vesamicol-insensitive pool of acetylcholine from a sympathetic-ganglion by ouabain. *J. Neurochem.* **61**:45–56.
 47. Prado, V. F., C. Martins-Silva, B. M. de Castro, R. F. Lima, D. M. Barros, E. Amaral, A. J. Ramsey, T. D. Sotnikova, M. R. Ramirez, H. G. Kim, J. I. Rossato, J. Koenen, H. Quan, V. R. Cota, M. F. Moraes, M. V. Gomez, C. Guatimosim, W. C. Wetsel, C. Kushmerick, G. S. Pereira, R. R. Gainetdinov, I. Izquierdo, M. G. Caron, and M. A. Prado. 2006. Mice deficient for the vesicular acetylcholine transporter are myasthenic and have deficits in object and social recognition. *Neuron* **51**:601–612.
 48. Prado, V. F., M. A. M. Prado, and S. M. Parsons. 2008. VACHT. UCSD-Nature Molecule Pages. doi:10.1038/mp.a002796.01.
 49. Rempe, D., G. Vangeison, J. Hamilton, Y. Li, M. Jepson, and H. J. Federoff. 2006. Synapsin I Cre transgene expression in male mice produces germline recombination in progeny. *Genesis* **44**:44–49.
 50. Ribeiro, F. M., J. Alves-Silva, W. Volkandt, C. Martins-Silva, H. Mahmud, A. Wilhelm, M. V. Gomez, R. J. Rylett, S. S. Ferguson, V. F. Prado, and M. A. Prado. 2003. The hemicholinium-3 sensitive high affinity choline transporter is internalized by clathrin-mediated endocytosis and is present in endosomes and synaptic vesicles. *J. Neurochem.* **87**:136–146.
 51. Ribeiro, F. M., S. A. Black, S. P. Cregan, V. F. Prado, M. A. Prado, R. J. Rylett, and S. S. Ferguson. 2005. Constitutive high-affinity choline transporter endocytosis is determined by a carboxyl-terminal tail dileucine motif. *J. Neurochem.* **94**:86–96.
 52. Ribeiro, F. M., S. A. Black, V. F. Prado, R. J. Rylett, S. S. Ferguson, and M. A. Prado. 2006. The “ins” and “outs” of the high-affinity choline transporter CHT1. *J. Neurochem.* **97**:1–12.
 53. Richards, D. A., C. Guatimosim, S. O. Rizzoli, and W. J. Betz. 2003. Synaptic vesicle pools at the frog neuromuscular junction. *Neuron* **39**:529–541.
 54. Song, H., G. Ming, E. Fon, E. Bellocchio, R. H. Edwards, and M. Poo. 1997. Expression of a putative vesicular acetylcholine transporter facilitates quantal transmitter packaging. *Neuron* **18**:815–826.
 55. Sudhof, T. C. 2004. The synaptic vesicle cycle. *Annu. Rev. Neurosci.* **27**:509–547.
 56. Sun, Y. A., and M. M. Poo. 1985. Non-quantal release of acetylcholine at a developing neuromuscular synapse in culture. *J. Neurosci.* **5**:634–642.
 57. Tucek, S. 1985. Regulation of acetylcholine synthesis in the brain. *J. Neurochem.* **44**:11–24.
 58. Vaca, K., and G. Pilar. 1979. Mechanisms controlling choline transport and acetylcholine synthesis in motor nerve terminals during electrical stimulation. *J. Gen. Physiol.* **73**:605–628.
 59. Van der Kloot, W. 1986. 2-(4-Phenylpiperidino)cyclohexanol (AH5183) decreases quantal size at the frog neuromuscular junction. *Pflügers Arch.* **406**:83–85.
 60. Van der Kloot, W. 2003. Loading and recycling of synaptic vesicles in the Torpedo electric organ and the vertebrate neuromuscular junction. *Prog. Neurobiol.* **71**:269–303.
 61. Vyskocil, F., and P. Illes. 1977. Non-quantal release of transmitter at mouse neuromuscular junction and its dependence on the activity of Na⁺-K⁺-ATP-ase. *Pflügers Arch.* **370**:295–297.
 62. Wang, Y. M., R. R. Gainetdinov, F. Fumagalli, F. Xu, S. R. Jones, C. B. Bock, G. W. Miller, R. M. Wightman, and M. G. Caron. 1997. Knockout of the vesicular monoamine transporter 2 gene results in neonatal death and supersensitivity to cocaine and amphetamine. *Neuron* **19**:1285–1296.
 63. Whitton, P. S., I. G. Marshall, and S. M. Parsons. 1986. Reduction of quantal size by vesamicol (AH5183), an inhibitor of vesicular acetylcholine storage. *Brain Res.* **385**:189–192.
 64. Yang, H., and S. Kunes. 2004. Nonvesicular release of acetylcholine is required for axon targeting in the *Drosophila* visual system. *Proc. Natl. Acad. Sci. USA* **101**:15213–15218.
 65. Zhu, H., J. S. Duerr, H. Varoqui, J. R. McManus, J. B. Rand, and J. D. Erickson. 2001. Analysis of point mutants in the *Caenorhabditis elegans* vesicular acetylcholine transporter reveals domains involved in substrate translocation. *J. Biol. Chem.* **276**:41580–41587.